Electronic Supporting Information (ESI)

New Efficient (Thio)acetalized Fullerene Monoadducts for Organic Solar Cells: Characterization Based on Solubility, Mobility Balance, and Dark Current

Tsubasa Mikie, Akinori Saeki, [*] Hiroyuki Masuda, Naohiko Ikuma, Ken Kokubo,[*] and Shu Seki[*]

Department of Applied Chemistry, Graduate School of Engineering, Osaka University, 2-1 Yamadaoka,

Suita, Osaka 565-0871, Japan.

*E-mail: saeki@chem.eng.osaka-u.ac.jp (A.S.)

kokubo@chem.eng.osaka-u.ac.jp (K.K.)

seki@chem.eng.osaka-u.ac.jp (S.S.)

Experimental.

Materials and Synthesis. Regioregular P3HT, fullerenes (C_{60} and PCBM), and solvents were purchased from Aldrich Inc., Frontier Carbon Inc., and Kishida Chemical Inc., respectively, and were used as received. Acetalized fullerenes **SAF** and **SAF$_n$** (n = 5-7) were synthesized in the same way with our previous report. [S1] Thioacetalized fullerene **STAF$_n$** (n = 5-7) was synthesized by the reaction of 2 equivalent of the dithiols $HS(CH_2)_nSH$ (n = 2, 3, 4) with cyclohexanone-fused fullerene **1** in presence of $TiCl_4$ as the catalyst. The structures of **STAF$_n$** (n = 5-7) were determined by ^1H and ^{13}C NMR analysis and MALDI-TOF-MS spectroscopy. Reduction potentials E_1^{red} standardized by Fc/Fc$^+$ couple were evaluated by cyclic voltammetry using an Ag/AgCl electrode and Pt as the working and counter electrode in *o*-dichlorobenzene (DCB), respectively. The lowest unoccupied molecular orbital (LUMO) levels were calculated from E_1 using LUMO level $= -e$ ($E_1^{red} + 4.8$). [S2]

Thioacetalized fullerene with 5-membered ring: **STAF$_5$**

^1H NMR (270 MHz, CS_2/CDCl$_3$) δ=3.47-3.63 (m, 2H, 2H, 4H), 4.15 (s, 2H); ^{13}C NMR (150 MHz, *o*DCB-d$_4$) δ=37.35, 41.26, 44.04, 54.14, 64.74, 64.82, 66.36, 136.27, 136.34, 140.93, 140.96, 142.29, 142.72, 142.74, 142.75, 142.77, 143.21, 145.37, 145.39, 145.98, 146.05, 146.07, 146.12, 146.23, 146.55, 146.90, 147.08, 147.11, 147.17, 148.31, 148.35, 156.81, 157.53; FAB MS, calculated for $C_{66}H_{10}S_2$ [M]$^+$, 866.0224, found 866.0206.

Thioacetalized fullerene with 6-membered ring: **STAF$_6$**

^1H NMR (270 MHz, CS_2/CDCl$_3$) δ2.23 (tt, 2H), 3.20 (m, 4H), 3.42 (m, 2H), 3.53 (m, 2H), 4.14(s, 2H); ^{13}C NMR (150 MHz, *o*DCB-d$_4$) δ25.40, 27.62, 35.34, 38.63, 49.41, 50.00, 63.31, 64.86, 135.64, 135.76, 140.22, 141.56, 141.59, 141.95, 142.02, 142.06, 142.48, 142.54, 143.21, 144.70, 145.11, 145.37, 145.39, 145.43, 145.52, 145.89, 146.16, 146.20, 146.35, 146.44, 147.62, 147.67, 156.22, 157.07; FAB MS, calculated for $C_{67}H_{12}S_2$ [M]$^+$, 880.0451, found 880.0480.

Thioacetalized fullerene with 7-membered ring: **STAF$_7$**

^1H NMR (270 MHz, CS_2/CDCl$_3$) δ=2.13 (m, 4H), 3.03 (m, 4H), 3.23 (m, H), 3.48(m, 2H), 3.80 (s, 2H); ^{13}C NMR (67.5 MHz, *o*DCB-d$_4$) δ=23.95, 32.83, 35.93, 40.88, 52.48, 60.24, 65.13, 136.28, 140.88, 140.91, 142.23, 142.25, 142.70, 142.75, 143.17, 143.20, 143.24, 243.92, 145.37, 145.41, 145.80, 145.99, 146.05, 146.08, 146.11, 146.24, 146.61, 146.86, 146.87, 147.04, 147.11, 148.30, 148.35, 157.07, 158.19; FAB MS, calculated for $C_{68}H_{14}S_2$ [M]$^+$, 894.0583, found 894.0560.

Organic photovoltaic cell (OPV).

Normal cell.[S3] P3HT and S(T)AFs were dissolved in 1.5 wt% DCB solution separately (1:1 wt ratio, 1.95 g / mL for each). A PEDOT:PSS layer was cast onto the cleaned ITO layer by spin-coating after passing through a 0.45 μm filter. The substrate was annealed on a hot plate at 120 °C for 10 min. After the substrate was annealed on a hot plate at 180 °C for 10 min, the DCB solution was then casted on top of the PEDOT:PSS buffer layer in a nitrogen glove box by spin-coating at 1400 rpm for 15 s after passing through a 0.2 mm filter. The thickness was around 200 nm. A cathode consisting of 20 nm Ca and 100 nm Al layers was sequentially deposited through a shadow mask on top of the active layers by thermal evaporation in a vacuum chamber. The resulting device configuration was ITO (120-160 nm)/PEDOT:PSS (45-60 nm)/active layer (ca. 200 nm)/Ca (20 nm)/Al (100 nm) with an active area of 7.1 mm^2.

Inverted cell. [S4, S5] A ZnO layer was fabricated onto a cleaned ITO layer by spin-coating of ZnO precursor solution (0.1 g/ml zinc acetate dihydrate and 0.028 g/ml ethanolamine in 2-methoxyethanol). The substrate was annealed on a hot plate at 200 °C for 30 min. An active layer consisting of polymer and fullerene was cast on top of the ZnO layer in a nitrogen glove box by spin-coating. The thickness was controlled by changing the rotation speed and measured by a surface profiler, an ULVAC model Dektak 150. An anode consisting of 10 nm MoO$_x$ and 100 nm Ag layers was sequentially deposited through a shadow mask on top of the active layers by thermal evaporation in a vacuum chamber. The resulting device configuration was ITO (120-160 nm)/ZnO(30 nm)/active layer /MoO$_x$ (10 nm)/Ag (100 nm) with an active area of 7.1 mm^2.

Evaluation. Current-voltage (*J-V*) curves were measured using a source-measure unit (ADCMT Corp., 6241A) under AM 1.5 G solar illumination at 100 mW cm^{-2} (1 sun, monitored by a calibrated standard cell, Bunko Keiki SM-250KD) from a 300 W solar simulator (SAN-EI Corp., XES-301S). The EQE spectra were measured by a Bunko Keiki model BS-520BK equipped with a Keithley model 2401 source meter. The monochromated light power was calibrated by a silicon photovoltaic cell, Bunko Keiki model S1337-1010BQ. Atomic force microscopy (AFM) observations were performed by a Seiko Instruments Inc. model Nanocute OP and Nanonavi II.

Space-charge limited current (SCLC). The device structures of SCLC were the ITO/PEDOT:PSS/active layer (ca. 200 nm)/Au for hole, and Al/Active layer (ca. 230 nm)/LiF/Al for electron, respectively. The other procedures are same with the OPV device fabrication. The active layer (blend of P3HT and fullerene) was prepared under the optimized condition. The hole or electron mobility was determined by fitting the J-V curve into Mott-Gurney law:[S6-S8]

$$j = \frac{9\varepsilon\varepsilon_0\mu V^2}{8d^3} \qquad \text{(S1)}$$

where ε_0 is the permittivity of free space, ε_r is the dielectric constant of the material, μ is the hole (or electron) mobility, V is the voltage drop across the device, and d is the thickness of the layer.

Surface energy (SE). Contact angles (θ) of fullerenes and P3HT were measured using water and glycerol droplets. The surface free energy (SFE) was calculated according to Kaelble–Uy theory[S9] given by

$$\gamma_L\left(1+\cos\theta\right) = 2\sqrt{\gamma_S^d\gamma_L^d} + 2\sqrt{\gamma_S^p\gamma_L^p} \qquad \text{(S1)}$$

, where γ_L and γ_S are SFEs of liquid and solid, respectively.

Crystallographic Data by Single Crystal X-Ray Diffraction (XRD).

A brown platelet crystal of $C_{68}H_{14}S_2$ having approximate dimensions of 0.40 x 0.15 x 0.05 mm was mounted on a glass fiber. All measurements were made on a Rigaku RAXIS RAPID imaging plate area detector with graphite monochromated Cu-Kα radiation.

Indexing was performed from 3 oscillations that were exposed for 150 seconds. The crystal-to-detector distance was 127.40 mm.

Cell constants and an orientation matrix for data collection corresponded to a primitive orthorhombic cell with dimensions:

a = 9.97592(18) Å

b = 19.8174(4) Å

c = 20.1513(4) Å

V = 3983.85(13) Å^3

For Z = 4 and F.W. = 894.98, the calculated density is 1.492 g/cm^3. The systematic absences of:

h00: $h \pm 2n$

0k0: $k \pm 2n$

00l: $l \pm 2n$

uniquely determine the space group to be: $P2_12_12_1$ (#19)

The data were collected at a temperature of -150 $\pm$ 1^{O}C to a maximum 2θ value of 143.5^O. A total of 96 oscillation images were collected. A sweep of data was done using ω scans from 80.0 to 260.0^O in 15.0^O step, at χ=54.0^O and ϕ = 0.0^O. The exposure rate was 30.0 [sec./^{O}]. A second sweep was performed using ω scans from 80.0 to 260.0^O in 15.0^O step, at χ=54.0^O and ϕ = 60.0^O. The exposure rate was 30.0 [sec./^{O}]. Another sweep was performed using ω scans from 80.0 to 260.0^O in 15.0^O step, at χ=54.0^O and ϕ = 120.0^O. The exposure rate was 30.0 [sec./^{O}]. Another sweep was performed using ω scans from 80.0 to 260.0^O in 15.0^O step, at χ=54.0^O and ϕ = 180.0^O. The exposure rate was 30.0 [sec./^{O}].

Another sweep was performed using ω scans from 80.0 to 260.0^O in 15.0^O step, at χ=54.0^O and ϕ = 240.0^O. The exposure rate was 30.0 [sec./^{O}]. Another sweep was performed using ω scans from 80.0 to 260.0^O in 15.0^O step, at χ=54.0^O and ϕ = 320.0^O. The exposure rate was 30.0 [sec./^{O}]. Another sweep was performed using ω scans from 80.0 to 260.0^O in 15.0^O step, at χ=20.0^O and ϕ = 20.0^O. The exposure rate was 30.0 [sec./^{O}]. Another sweep was performed using ω scans from 80.0 to 260.0^O in 15.0^O step, at χ=20.0^O and ϕ = 120.0^O. The exposure rate was 30.0 [sec./^{O}]. The crystal-to-detector distance was 127.40 mm. Readout was performed in the 0.100 mm pixel mode.

Empirical Formula	$C_{68}H_{14}S_2 \cdot C_7H_8$
Formula Weight	987.12
Crystal Color, Habit	brown, platelet
Crystal Dimensions	0.40 X 0.15 X 0.05 mm
Crystal System	orthorhombic
Lattice Type	Primitive
Indexing Images	3 oscillations @ 150.0 seconds
Detector Position	127.40 mm
Pixel Size	0.100 mm
Lattice Parameters	a = 9.97592(2) Å
	b = 19.8174(4) Å
	c = 20.1513(4) Å
	V = 3983.85(2) Å^3
Space Group	$P2_12_12_1$ (#19)
Z value	4
D_{calc}	1.492 g/cm^3
F_{000}	1816.00
μ(CuKα)	16.124 cm^{-1}
Residuals: R1 (I>2.00σ(I))	0.0693
Residuals: R (All reflections)	0.0981
Residuals: wR2 (All reflections)	0.1923

Supporting References.

[S1]   K. Kokubo, H. Masuda, N. Ikuma, T. Mikie, T. Oshima. *Tetrahedron Lett*, **2013**, *54*, 3510.

[S2]   M. S. Liu, X. Jiang, S. Liu, P. Herguth, A. K.-Y. Jen *Macromolecules* **2002**, *35*, 3532.

[S3]   A. Saeki, M. Tsuji, S. Seki, *Adv. Energy Mater.* **2011**, *1*, 661.

[S4]   A. Saeki, M. Tsuji, S. Yoshikawa, A. Gopal, S. Seki, *J. Mater. Chem. A* **2014**, *2*, 6075.

[S5]   Y. Sun, J. H. Seo, C. J. Takacs, J. Seifter, A. J. Heeger, *Adv. Mater.* **2011**, *23*, 1679.

[S6]   P. W. M. Blom, M. J. M. de Jong, J. J. M. Vleggaar, *Appl. Phys. Lett.* **1996**, *68*, 3308.

[S7]   C. Melzer, E. J. Koop, V. D. Mihailetchi, P. W. M. Blom, *Adv. Funct. Mater.* **2004**, *14*, 865.

[S8]   D. H. Dunlap, P. E. Parris, V. M. Kenkre, *Phys. Rev. Lett.*, **1996**, *77*, 542.

[S9]   D. H. Kaelble, K. C. Uy, *J. Adhesion* **1970**, *2*, 50.

Supporting Tables.

Table S1. Reduction potentials of **SDOF$_n$** in DCB.

Compound	E^1_{red} / V [a]	E^2_{red} / V [a]	E^3_{red} / V [a]	LUMO / eV [b]
STAF$_5$	−1.20	−1.57	−2.09	−3.60
STAF$_6$	−1.22	−1.58	−2.08	−3.58
STAF$_7$	−1.22	−1.58	−2.09	−3.58

[a] Reduction potentials E_{red} = 0.5 (E^{ox}_p + E^{red}_p) were measured versus Ag/AgCl reference electrode and standardized to Fc/Fc$^+$ couple E_{Fc/Fc^+} = +0.224 V versus Ag/Ag$^+$ (DCB) in 0.1 mM DCB with 0.1 M ^{n}Bu$_4$PF$_6$ as supporting electrolyte. Scan rate was 100 mV/s. [b] Calculated from E_1 using LUMO level = $-e$ (E$^1_{red}$ + 4.8).

Table S2. Influence of polymer:fullerene (D/A) ratios on photovoltaic properties of the P3HT:**SAF$_7$** devices.

Ratio (P3HT:**SAF$_7$**)	J_{sc} / mAcm^{-2}	V_{oc} / V	FF	PCE / %
1:0.8	7.87	0.66	0.62	3.22
1:1	8.43	0.64	0.66	3.52
1:1.2	7.62	0.49	0.46	1.70

Table S3. Contact angle (CA) and surface energy (SE) measurements.

Films	CA$_{glycerol}$ / °	CA$_{water}$ / °	SE / mJ cm^{-2}
1	80.98	95.99	25.5
SAF$_5$	27.16	40.75	57.6
SAF$_6$	68.83	74.54	29.9
SAF$_7$	70.71	84.14	29.8
STAF$_5$	59.72	70.07	35.9
STAF$_6$	61.12	64.98	36.9
STAF$_7$	59.82	65.31	37.0
PCBM	61.93	75.02	35.0
P3HT	101.73	106.6	10.1

Table S4. OPV outputs of PTB7:**SAF₇** (best values) processed from CB with DIO.

Cell	DIO / vol%	J_{sc} / mAcm^{-2}	V_{oc} / V	FF	PCE / %
Inverted [a]	0	5.46	0.74	0.35	1.41
Inverted [a]	1	8.57	0.74	0.39	2.48
Inverted [a]	3	13.34	0.76	0.57	5.84
Inverted [a]	5	11.91	0.78	0.60	5.56
Inverted [a]	7	11.95	0.78	0.61	5.65
Inverted [a]	10	11.47	0.77	0.56	4.95
Normal [b]	7	6.03	0.83	0.38	1.91

[a] Inverted cell (glass/ITO/ZnO/BHJ/MoO$_x$/Ag). [b] Normal cell (glass/ITO/PEDOT:PSS/BHJ/Ca/Al).

Supporting Figures.
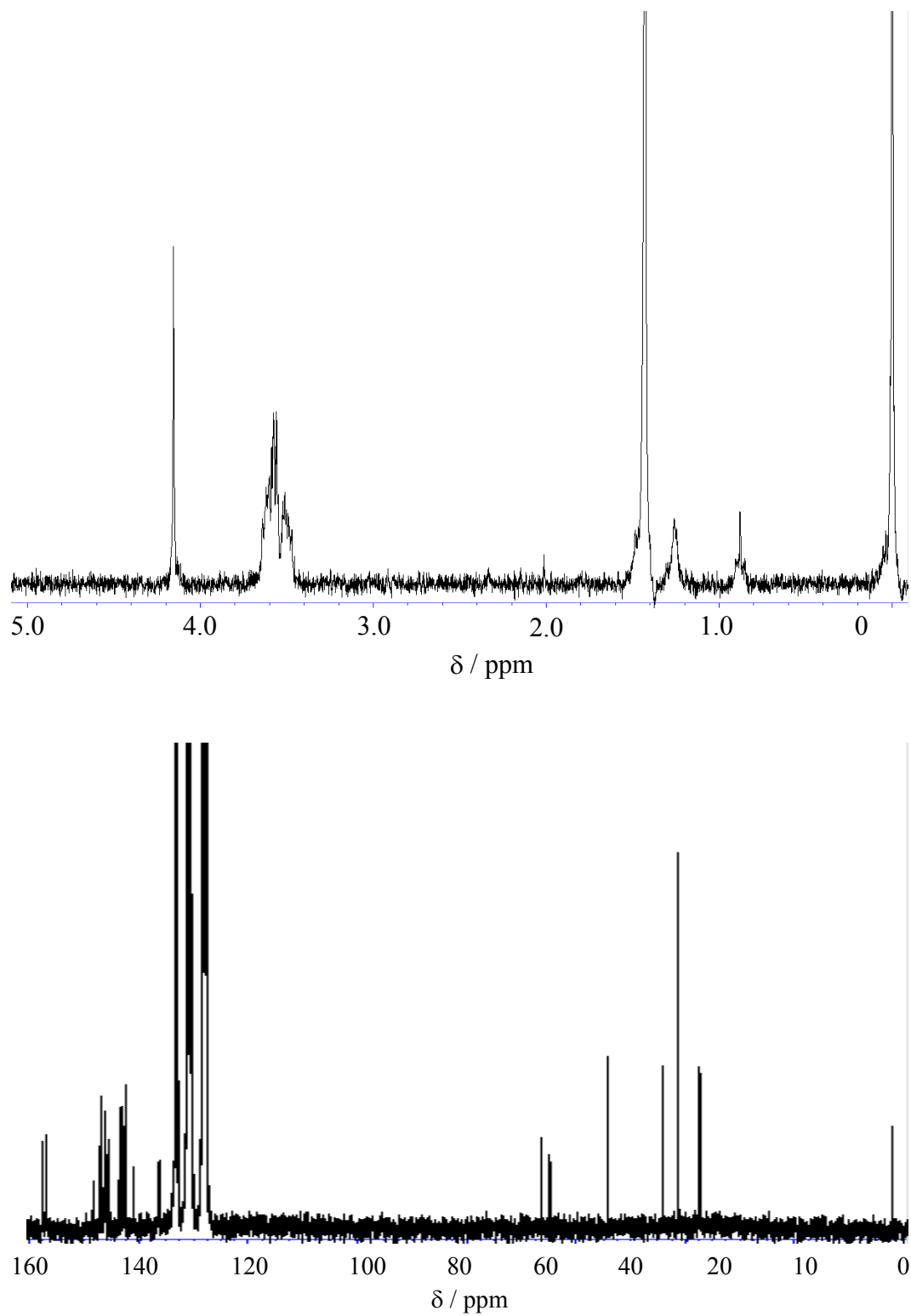
Figure S1. ¹H (upper) and ¹³C NMR spectra (lower) of **STAF₅**.
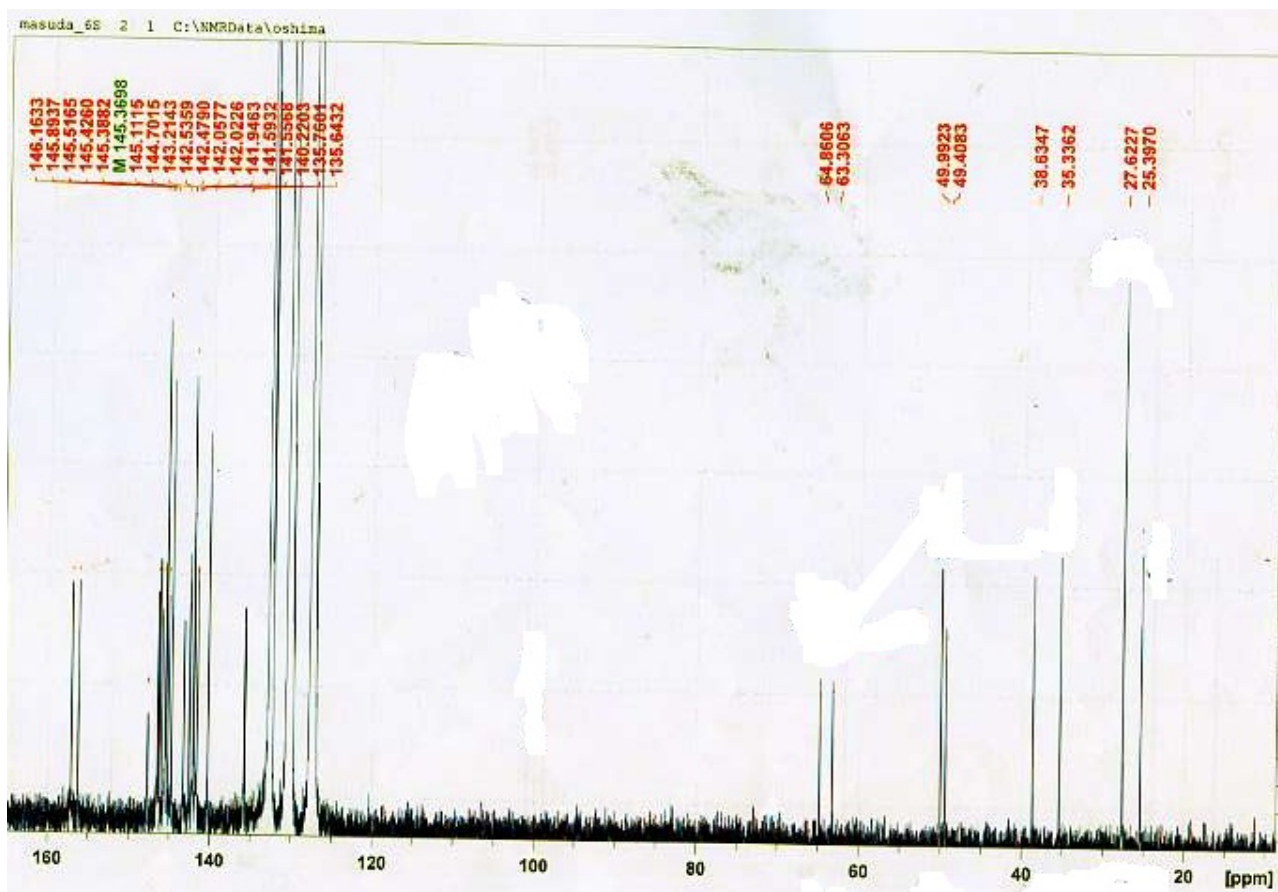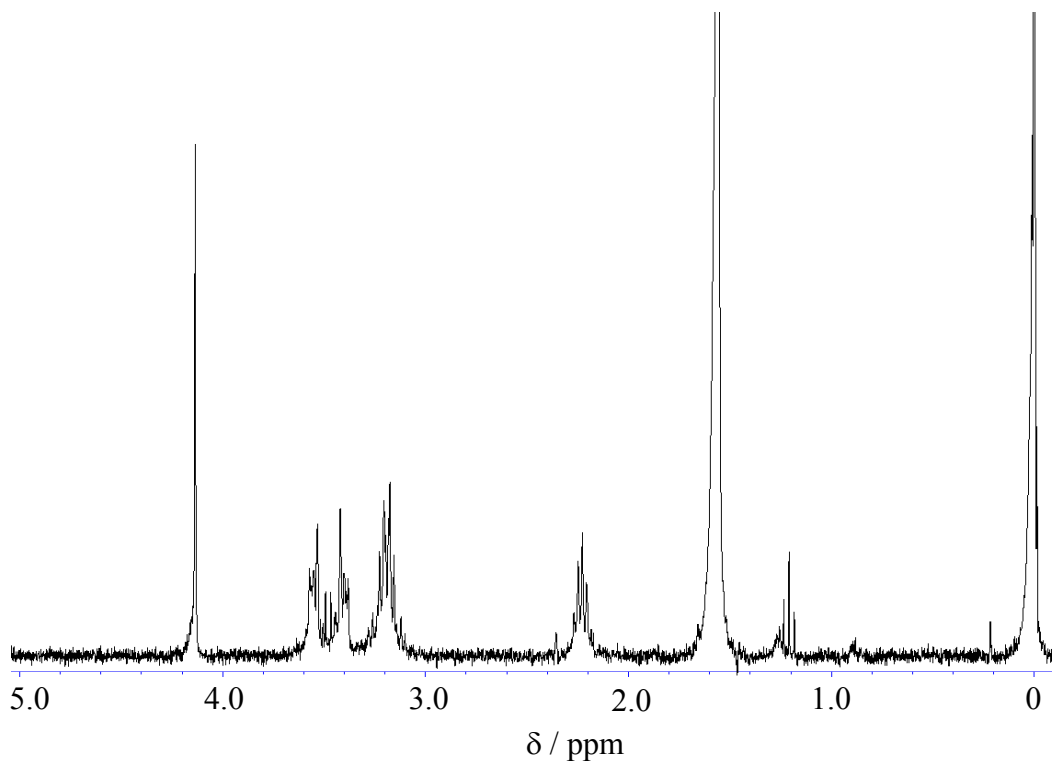
Figure S2. ^{1}H (upper) and ^{13}C NMR spectra (lower) of **STAF$_6$**.
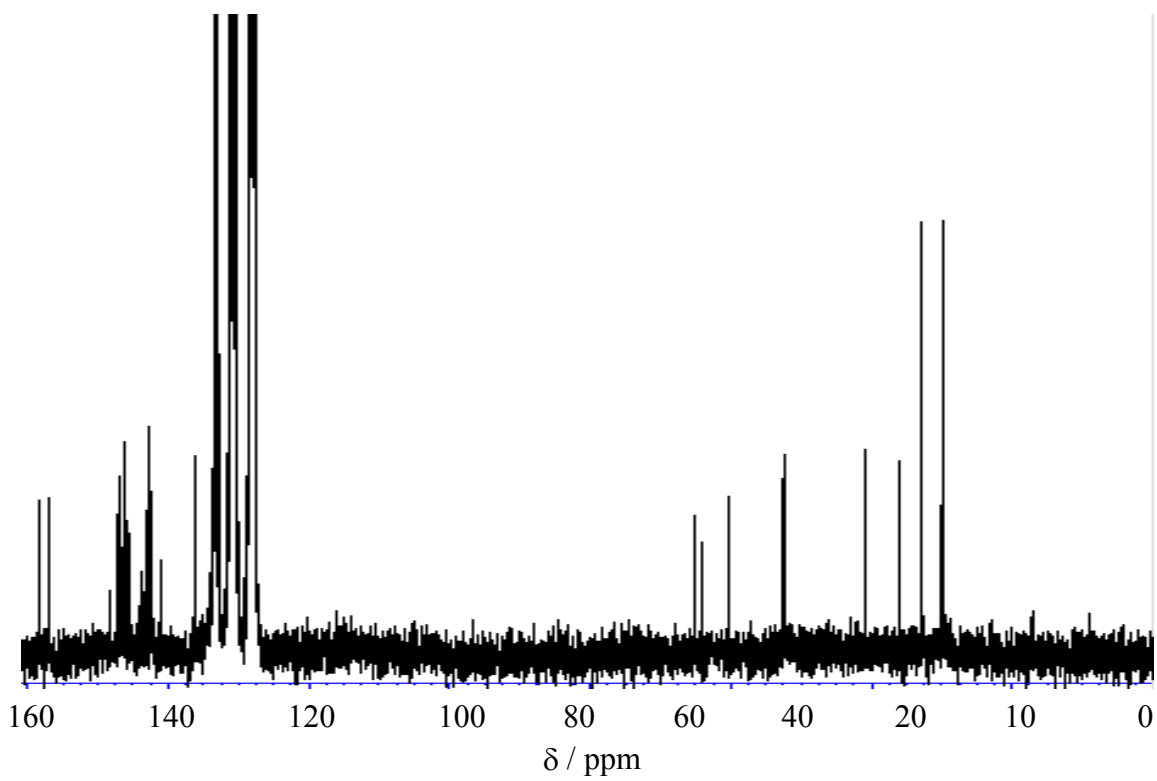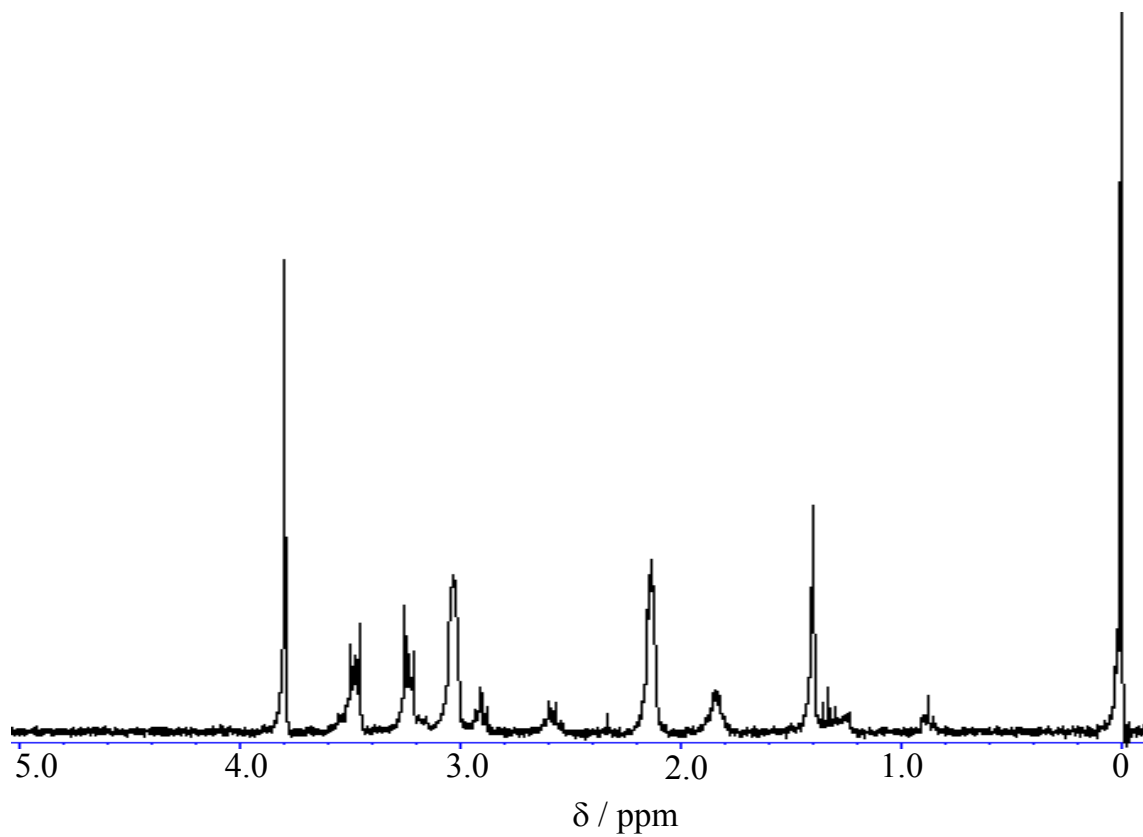
Figure S3. ^{1}H (upper) and ^{13}C NMR spectra (lower) of **STAF$_7$**.
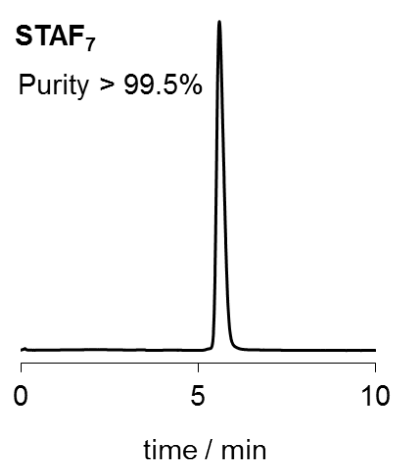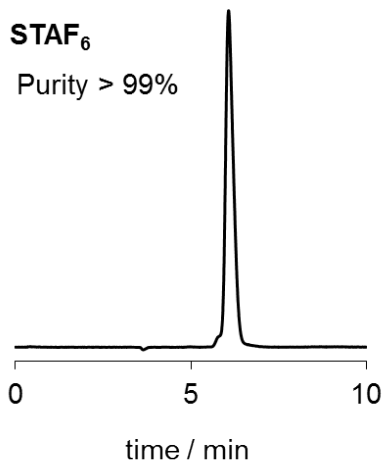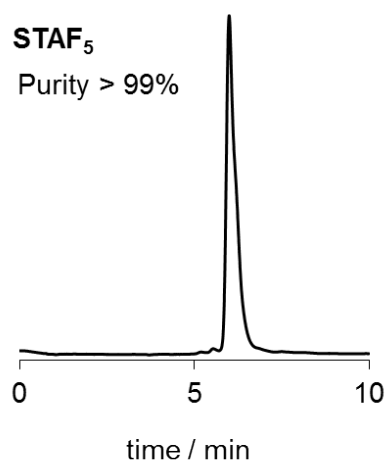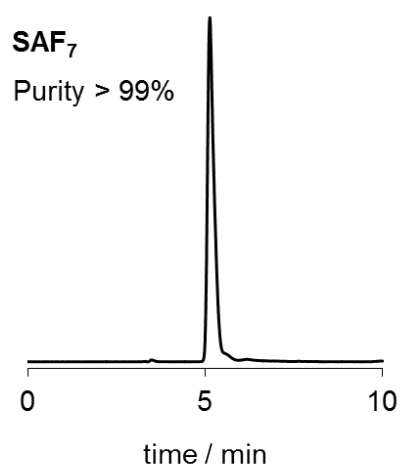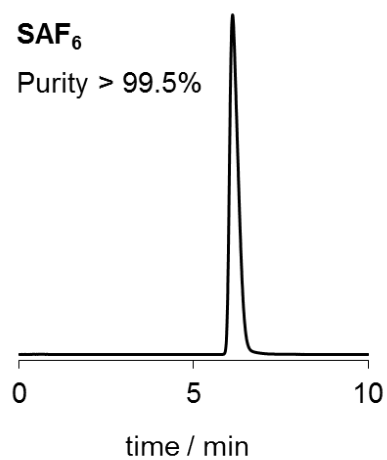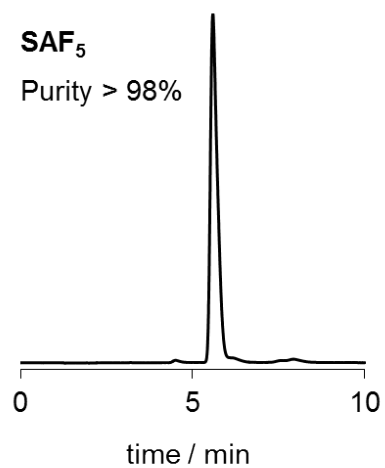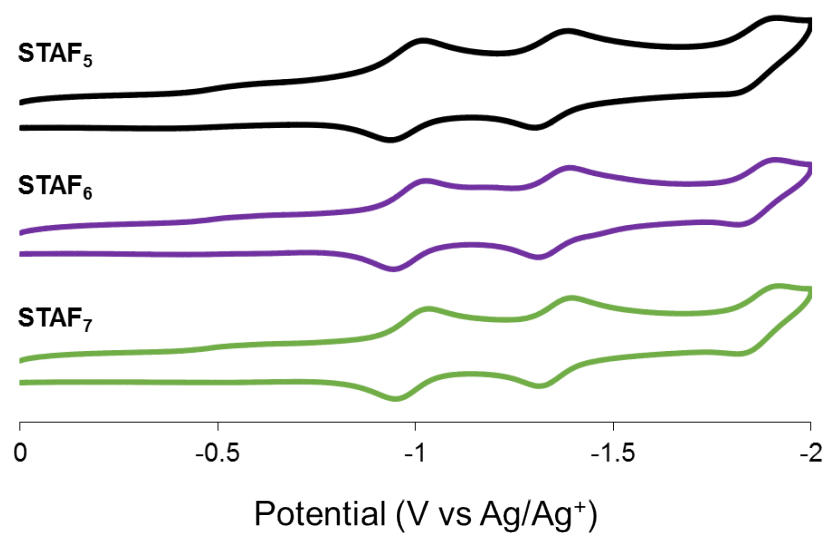
Figure S4. Purity of **STAFs** evaluated by HPLC.

Figure S5. Cyclic volotammograms of **STAF$_n$**.
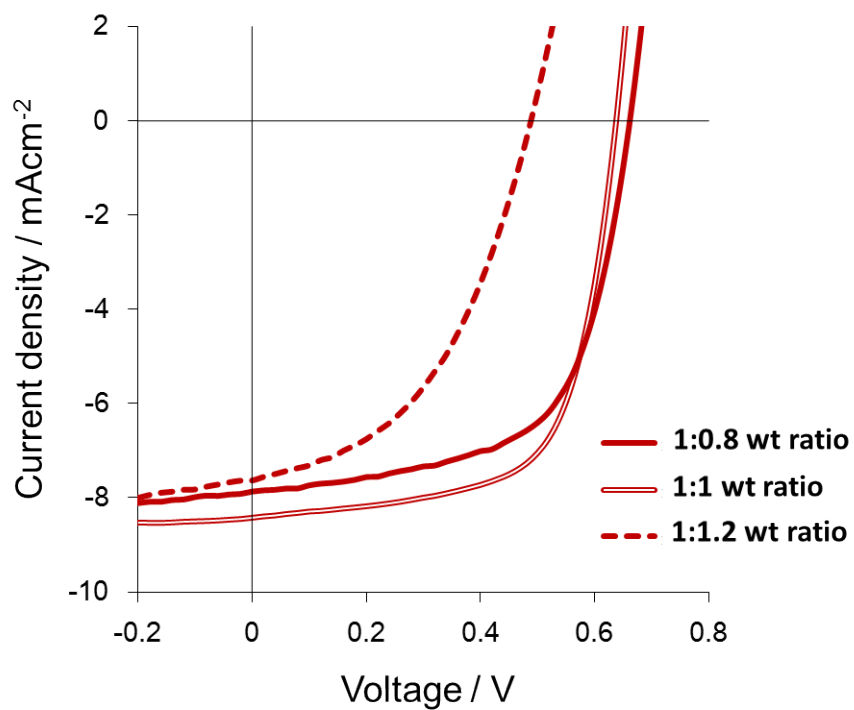
Figure S6. *J-V* curves of P3HT:**SAF$_7$** =1:0.8 (solid line), 1:1 (double line), and 1:1.2 (dotted line) normal cells processed from DCB under AM1.5G (100 mW cm^{-2}).

1	**SAF$_6$**	**SAF$_7$**	**STAF$_6$**	**STAF$_7$**	**PCBM**

top

RMS = 8.00 nm RMS = 5.71 nm RMS = 8.07 nm RMS = 3.25 nm RMS = 8.33 nm RMS = 8.43 nm
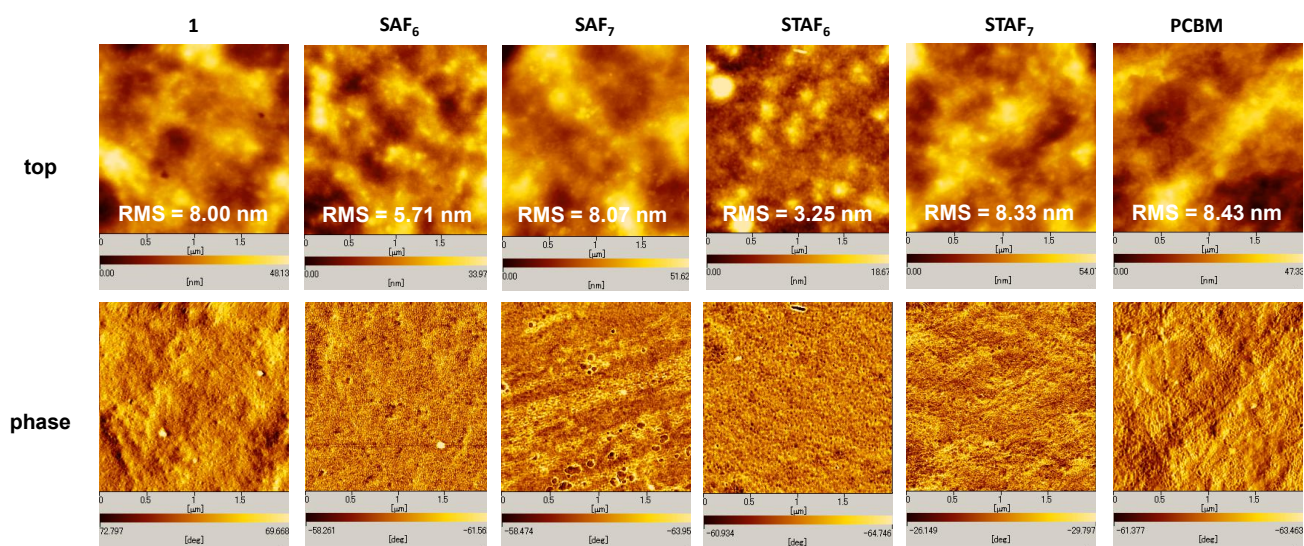
phase

Figure S7. Atomic force microscopy (AFM) topological (upper) and phase images (bottom) of P3HT:fullerenes at the best condition. The image size is 2 × 2 μm^2.
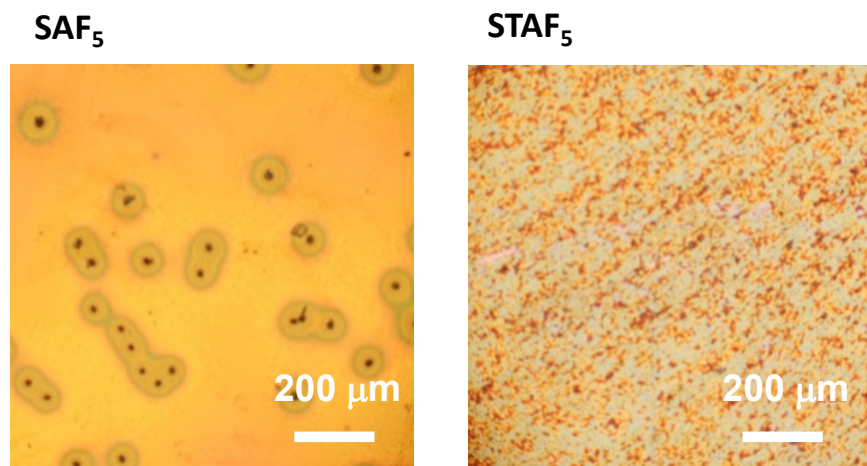
SAF₅

STAF₅

Figure S8. Optical microscope of the blend film of fullerenes **SAF₅** and **STAF₅** with P3HT.
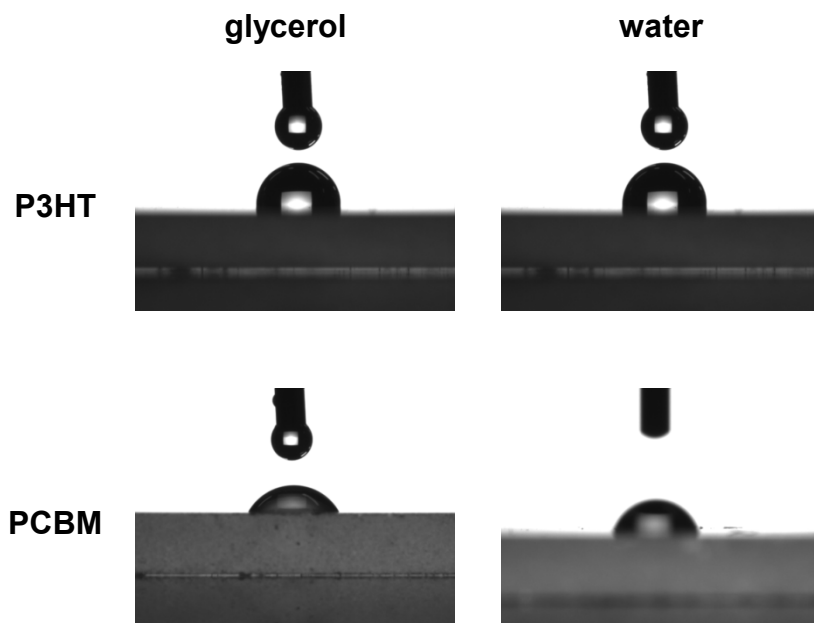
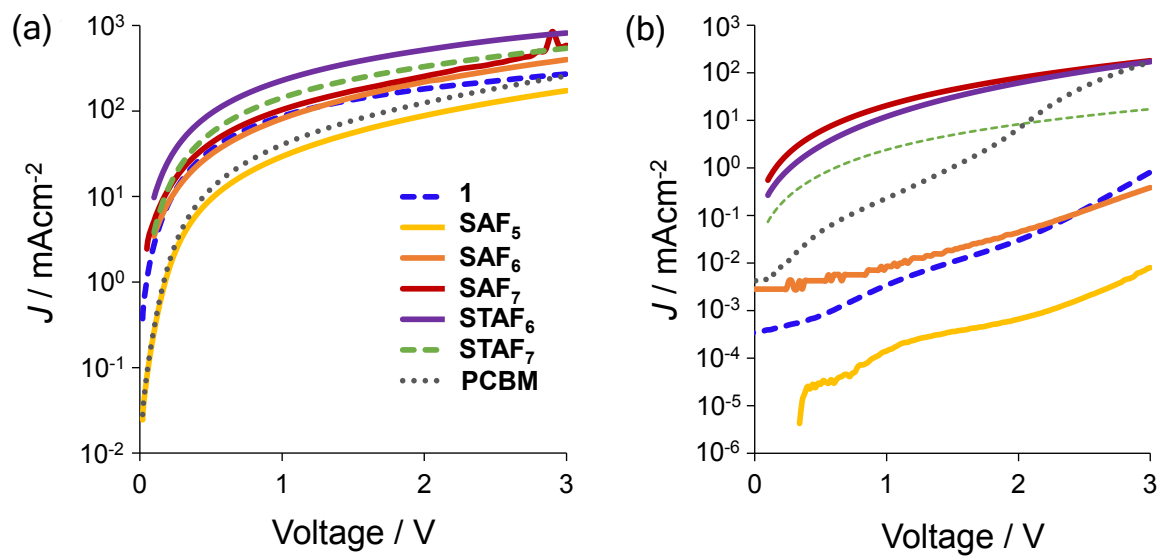**Figure S9.** Examples of contact angle measurement pictures.

Figure S10. SCLC *J-V* curves of P3HT:fullerenes (1:1 in wt%) under dark conditions using optimized device condition. (a) Hole- and (b) electron-only devices.
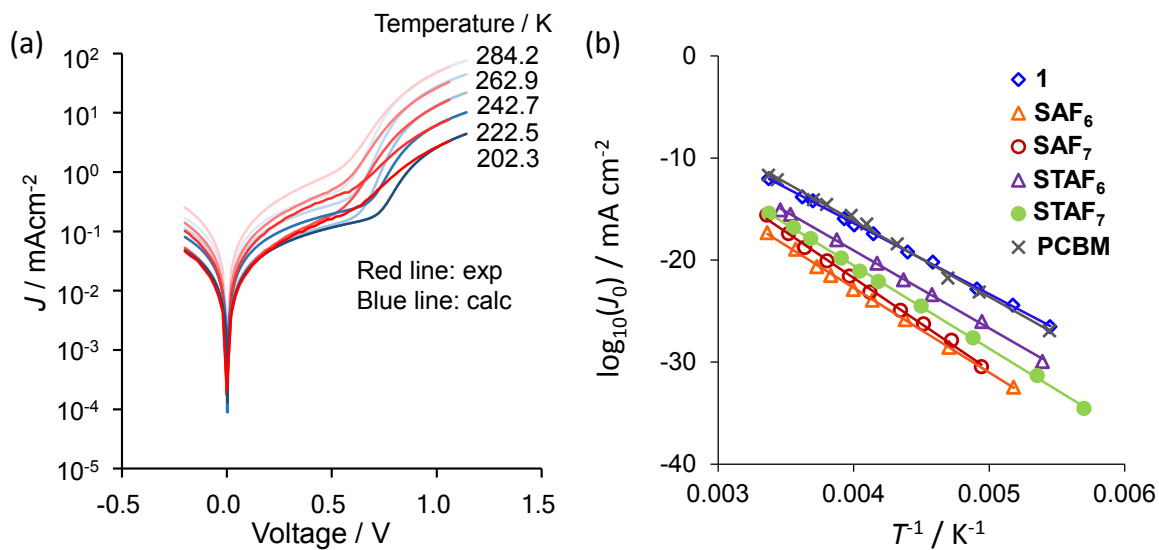
Figure S11. a) Dark currents of P3HT:**SAF$_7$** (1:1 in wt%) device at low temperature. b) Temperature dependence of dark current of P3HT:fullerne (1:1 in wt%) OPV.
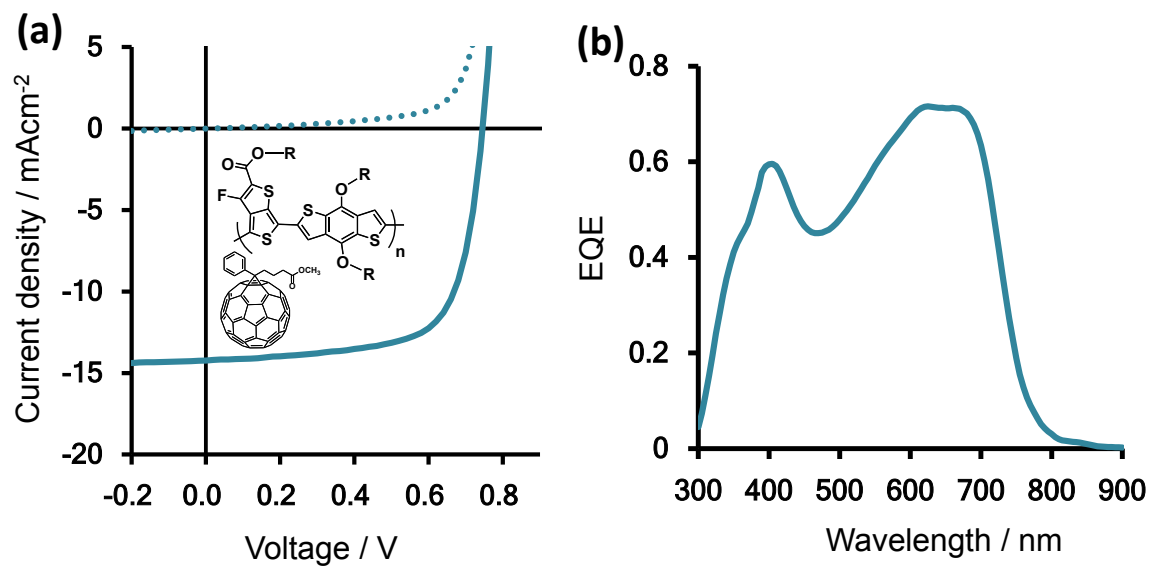
Figure S12. OPV output of PTB7:PCBM (1:1.5 wt%) inverted cell processed from CB with 3vol% DIO. (a) *JV* curves under AM1.5G (100 mW cm^{-2}, solid line) and dark (dotted line). The chemical structures are superimposed. (b) External quantum efficiency (EQE) spectrum of the corresponding device. The calculated J_{sc} is 14.23 mA cm^{-2}, consistent with the J_{sc} under one sun (13.96 mA cm^{-2}).
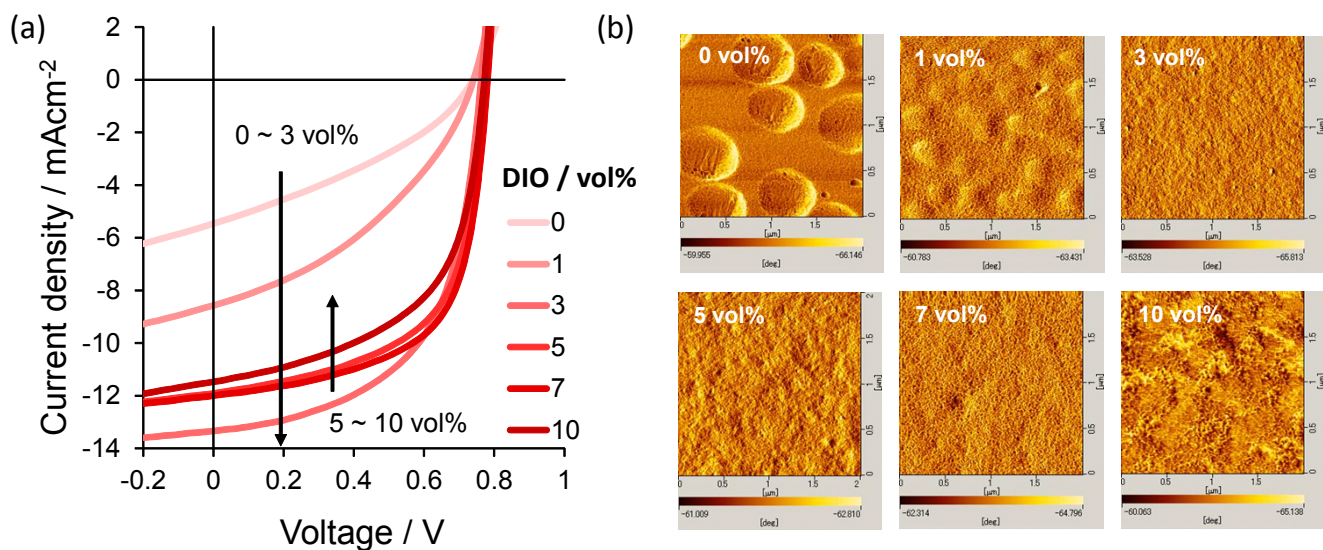
Figure S13. (a) *J-V* curve of PTB7:**SAF₇** (1:1.5 wt%) inverted cells processed from CB with various DIO concentration under AM1.5G (100 mW cm⁻²). (b) AFM phase images (2 × 2 μm²) of the films. The values indicate the DIO concentration.